iScience

CellPress
OPEN ACCESS

Article

Molecular and clonal evolution *in vivo* reveal a common pathway of distant relapse gliomas

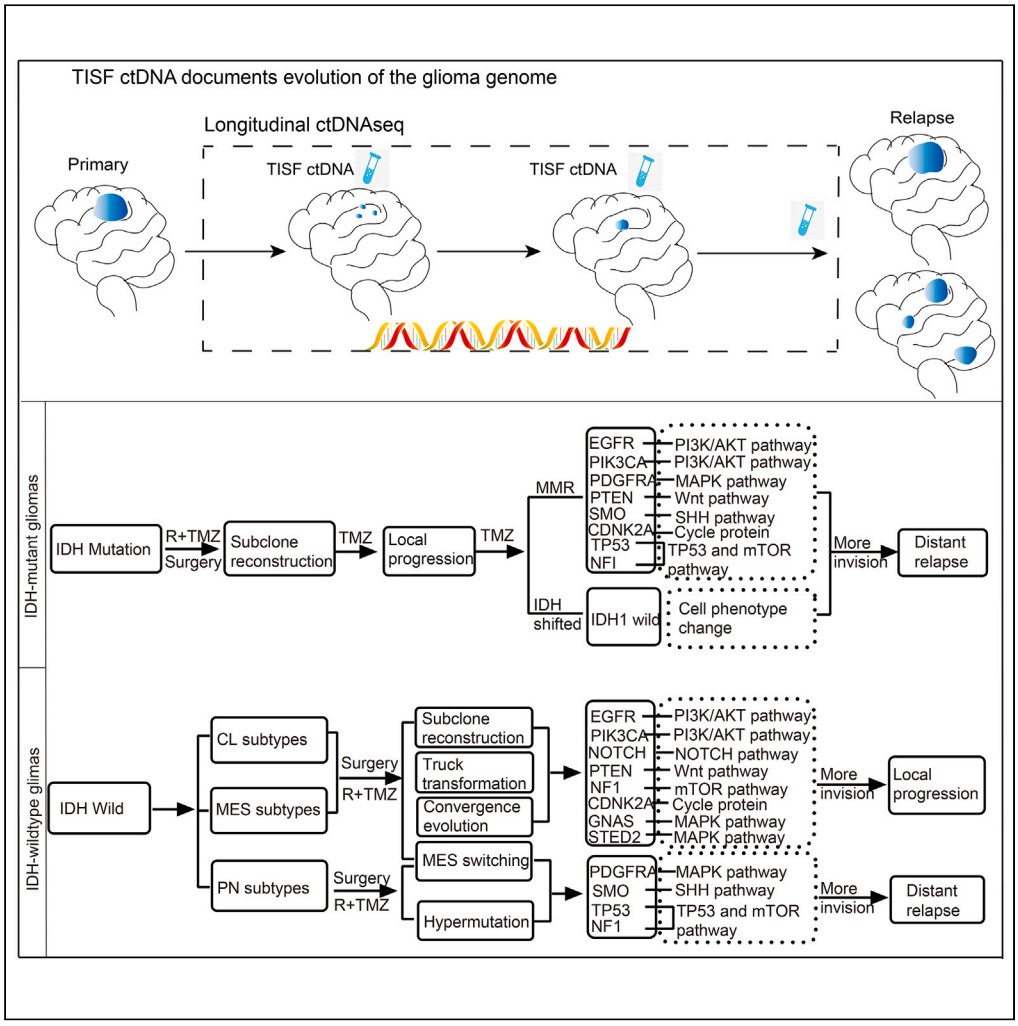

Guanzheng Liu, Chaojie Bu, Guangzhong Guo, ..., Tianxiao Li, Ming Li, Xingyao Bu

docliming@163.com (M.L.)
xingyaob@zzu.edu.cn (X.B.)

Highlights

Distant relapse gliomas may display a more aggressive genetic phenotype

MMR mutations and IDH transformation promote distant relapse in IDH-mutant gliomas

Different subtype glioblastomas have their own preferred evolution patterns

Multifocal glioma may originate from a monoclonal gene, undergo parallel evolution

Liu et al., iScience *26*, 107528
September 15, 2023
https://doi.org/10.1016/j.isci.2023.107528

iScience

CellPress
OPEN ACCESS

Article

Molecular and clonal evolution *in vivo* reveal a common pathway of distant relapse gliomas

Guanzheng Liu,[1,2,6] Chaojie Bu,[1,2,6] Guangzhong Guo,[1,2,6] Zhiyue Zhang,[1,2,6] Zhiyuan Sheng,[1,2] Kaiyuan Deng,[1,2] Shuang Wu,[1,2] Sensen Xu,[1,2] Yage Bu,[1,2] Yushuai Gao,[1,2] Meiyun Wang,[3] Gang Liu,[4] Lingfei Kong,[5] Tianxiao Li,[1,2] Ming Li,[1,2,*] and Xingyao Bu[1,2,7,*]

SUMMARY

The evolutionary trajectories of genomic alterations underlying distant recurrence in glioma remain largely unknown. To elucidate glioma evolution, we analyzed the evolutionary trajectories of matched pairs of primary tumors and relapse tumors or tumor *in situ* fluid (TISF) based on deep whole-genome sequencing data (ctDNA). We found that MMR gene mutations occurred in the late stage in IDH-mutant glioma during gene evolution, which activates multiple signaling pathways and significantly increases distant recurrence potential. The proneural subtype characterized by PDGFRA amplification was likely prone to hypermutation and distant recurrence following treatment. The classical and mesenchymal subtypes tended to progress locally through subclonal reconstruction, trunk genes transformation, and convergence evolution. EGFR and NOTCH signaling pathways and CDNK2A mutation play an important role in promoting tumor local progression. Glioma subtypes displayed distinct preferred evolutionary patterns. ClinicalTrials.gov, NCT05512325.

INTRODUCTION

Tumors typically harbor heterogeneous subclones with distinct genetic profiles. Analyzing subclonal evolution can provide insights into more effective therapeutic approaches.[1] The evolutionary dynamics underlying tumor progression and relapse are poorly understood. However, liquid biopsy, such as the use of circulating tumor DNA (ctDNA), offers new possibilities for understanding tumor evolution.[2] ctDNA is present in the early stage of tumor recurrence,[3,4] and ctDNA sequencing has shown promise in delineating the genomic landscape, subclonal architecture, and genetic evolution of tumors.[5,6]

Gliomas are the most common and aggressive type of primary brain tumors in adults. Despite the benefits from TMZ (temozolomide), recurrence inevitably occurs either locally (~80%) or distally (~20%), leading to fatal outcomes.[7] Previous work showed that 63% of gliomas display marked changes in molecular subtype at relapse, with 15% exhibiting hypermutation that may drive malignant progression.[8] TMZ-induced hypermutation is common in low-grade gliomas (LGGs) and linked to worse prognosis and distant recurrence.[9] Analysis of paired primary and recurrent glioblastomas suggests a shared early tumorigenic stage involving gains of chromosome 7 and losses of 9p or 10p, followed later by TERT promoter mutations.[10] Tumors recurred in distinct patterns, which depend on IDH mutation state and arise from changes in histological characteristics, somatic alterations, and microenvironment interactions.[11] However, the actual molecular trajectory *in vivo* between initial and relapse tumors has not been clearly elucidated, which is clinically significant for understanding the real-time molecular landscape and recurrence patterns. Actually, it is still challenging to study glioma evolution by detecting ctDNA in plasma and CSF.[12,13] Tumor shedding DNA into the CSF is influenced by tumor burden.[13] Our study demonstrated evolution trajectories differed markedly in distinct glioma subtypes with variant relapse patterns based on analysis of ctDNA.

Our preliminary studies show high concordance of shared mutations between TISF DNA and tumor tissue. TISF-ctDNA analysis can reveal real-time genomic evolution and characterize the genetic landscapes of recurrent gliomas, potentially with greater sensitivity than CSF-ctDNA.[14] Therefore, real-time monitoring

[1]Department of Neurosurgery, Zhengzhou University People's Hospital, Henan Provincial People's Hospital, Zhengzhou 450003, China

[2]Juha International Central Laboratory of Neurosurgery, Henan Provincial People's Hospital, Zhengzhou 450003, China

[3]Department of Radiology, Henan Provincial People's Hospital, Zhengzhou 450003, China

[4]Department of Center for Clinical Single Cell Biomedicine, Clinical Research Center, Department of Oncology, Henan Provincial People's Hospital, Zhengzhou University People's Hospital, Zhengzhou 450003, China

[5]Department of Pathology, Henan Provincial People's Hospital, Zhengzhou 450003, China

[6]These authors contributed equally

[7]Lead contact

*Correspondence: docliming@163.com (M.L.), xingyaob@zzu.edu.cn (X.B.)

https://doi.org/10.1016/j.isci.2023.107528

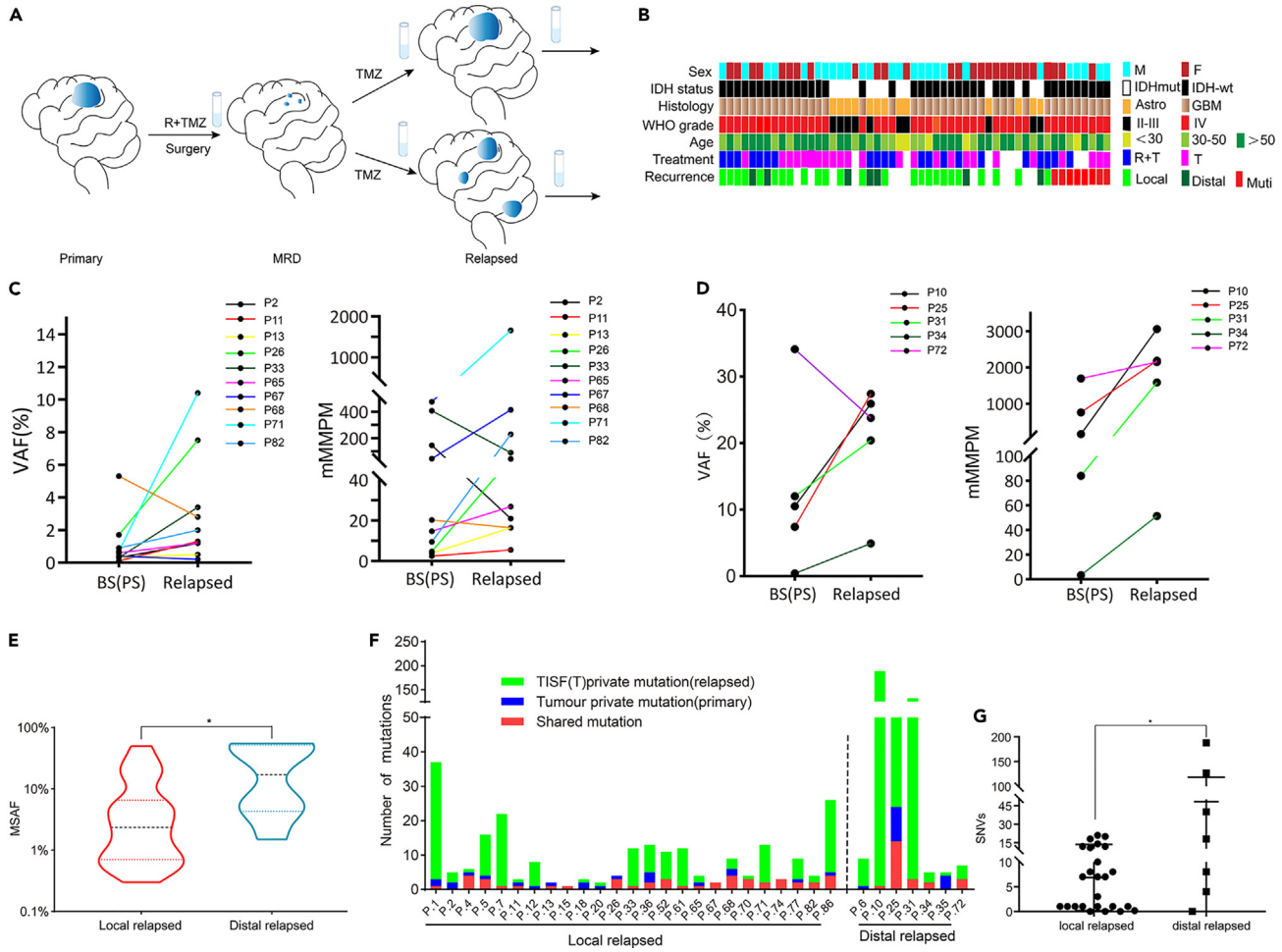

Figure 1. Clinical features of glioma patients

(A) Tracking the genetic changes of glioma patients with distinct relapse patterns based on ctDNA *in vivo*.

(B) Overview of clinical parameters.

(C and D) Evaluation of alterations in variant allele frequency (VAF) and mean mutant molecules per milliliter (mMMPM) indexes between relapse and baseline or progression TISF ctDNA. More alterations were observed in distant relapse tumors compared to local relapse tumors.

(E) Increased alterations in the maximum somatic allele frequency (MSAF) in distant relapse compared to local relapse tumors. $p < 0.05$.

(F) All shared mutations and some private mutations number between primary tumor and relapse TISF are shown.

(G) Higher variations in single-nucleotide variants (SNVs) in distant relapse tumors with more subclones compared to local relapse tumors. $p < 0.05$.

of gene evolution using TISF-ctDNA may provide insights into the molecular mechanisms of different recurrence patterns.

RESULTS

Clinical features of glioma patients

We collected longitudinal tumor tissue and matched TISF samples from 52 glioma patients and performed ctDNA sequencing (Figure 1A). This study included 44 patients: 12 (27.3%) with IDH-mutant and 32 (72.7%) with IDH-wildtype glioblastomas (GBMs). Eight had multifocal gliomas. Along with standard chemotherapy, 21 patients received radiotherapy. Here, we selected 32 patients with paired tumor and TISF samples. 7 had distant recurrence and 25 (3 with IDH-mutant) had local recurrence (Figure 1B).

Gliomas inevitably recur either locally or distally. To elucidate differences in evolutionary dynamics during treatment, we evaluated alterations in the variant allele frequency (VAF) and mean mutant molecules per milliliter (mMMPM) indexes in TISF-ctDNA between relapse and baseline or progression samples. Alterations were greater in distant vs. local relapse (Figures 1C and 1D). Similar results were seen for maximum

somatic allele frequency (MSAF) (Figure 1E). More subclones in distant relapse tumors showed additional mutations that were not found in the primary tumor, indicating greater heterogeneity during tumor evolution (Figures 1F and 1G). These results suggest that distant relapse tumors may display a more aggressive mutational phenotype.

Longitudinal mutational landscape of gliomas

To elucidate the mechanisms driving distinct evolution patterns at relapse in gliomas under therapy, we analyzed 44 untreated whole exomes from primary tumor:12 IDH-mutant astrocytomas and 32 IDH-wildtype GBMs. IDH-mutant astrocytomas harbored mutations in ATRX (50%, 6/12), TP53 (100%,12/12), PIK3CA (17%,2/12), NOTCH1 (17%,2/12) and CDNK2A (8%,1/12), along with IDH mutation. Meanwhile, we also detected CDK4 (8%,1/12) and MET (8%,1/12) amplification in IDH-mutant gliomas. We detected mutations known as oncogenic driver genes of glioblastoma.[15] IDH-wildtype GBMs exhibited mutations in PTEN (31%,10/32), NF1 (25%,8/32), TP53 (19%,6/32), EGFR (19%,6/32), PIK3CA (13%,4/32), PIK3R1 (13%, 10/32), and PTPN11 (9%,3/32), along with EGFR (31%,10/32), PDGFRA (9%, 3/32), and CDK4 (13%,4/32) amplifications. EGFR and PDGFRA amplification only occur in IDH-wild gliomas, unlike CDK4 and MET amplifications (Figures 2A and 2C).

To explore evolution from initial tumor to local recurrence in IDH-wildtype GBMs, we analyzed 22 patients with paired samples and identified alterations by ctDNA sequencing. Recurrence analysis found changes in known GBM drivers. EGFR mutant, which was observed in 19% of initial tumors (6/32) and 30% of recurrence samples (12/44). CDKN2A mutations rose from 3% (1/32) to 18% (8/44). NOTCH1 mutant, not a driver gene, displayed a rising prevalence in local recurrent samples (19%,5/44). And BRAF mutations, activating MAPK signaling,[16] rose from 6% (2/32) to 16% (7/44). GNAS mutations increased from 3% (1/32) to 16% (7/44). SETD2 mutations, integrating EZH2 and MAPK signaling, has been detected in 3% of initial (1/32) and 16% of recurrence samples (7/44). And PTEN and NF1 mutations had no obvious change during the progression of evolution. These findings suggest that key roles for RAS (EGFR, GNAS, BRAF, STED2), NOTCH signaling and cell cycle regulator (CDKN2A) in local recurrence (Figures 2A and 2B).

Analysis of seven distant recurrences (4 with IDH-mutant and 3 with IDH-wildtype) revealed DNA mismatch repair (MMR) gene mutations (5/14), primarily in distant recurrence. Two distant recurrences had >100 mutations, including MMR mutations consistent with a hypermutation genotype.[17] Co-mutation of TP53 and NF1 was more common in distant recurrence (6/14), as reported.[18] Major changes occurred in stem cell self-renewal and proliferation. Hedgehog (SMARCB1 and SMO, 5/14) and PDGFRA (5/14) signaling pathways were activated significantly, unlike local recurrence. Recently, Hedgehog (SHh) and PDGFRA signaling influence cancer progression and metastasis.[19–21] Furthermore, we found that the proneural (PN) subtype with PDGFRA amplification tended to distant recurrence (2/2), while the classical subtype favored local progression and recurrence (6/7) (Figures 2B and 2C). Multiple subclones during progression achieved invasion, metastasis and resistance. Glioma subtypes displayed preferred evolution patterns. These results provide hypotheses for distant recurrence events relevant to personalized therapy.

MMR mutations and IDH transformation promoted distant relapse in IDH-mutant gliomas

To elucidate the underlying molecular mechanisms driving distant recurrence in IDH-mutation astrocytomas, we performed whole exome sequencing of tumor and longitudinal matched TISF-ctDNA from 7 glioma patients. Four patients achieved distant relapse and three patients progressed locally. Patient 26 initially had been diagnosed with a right temporal lesion and underwent initial surgical resection, and received a histopathological diagnosis of WHO grade II astrocytoma. IDH:p.R132H, TP53:p.R273C and PIK3CA:p.Q546K were confirmed as driver genes in tumor tissue. Reoperation were performed when tumor recurred. These driver mutations were all detected in the relapse tissue (Figure 3A). Patient 86 underwent two operations as well. Further analysis revealed a number of subclonal mutations appeared in the relapse sample, but were not detected in the primary tumor. The pathological grade upgraded from WHO grade II to IV. IDH:p.R132H, TP53:p.R282W and ATRX:p.Q1319Kfs*27 as driver genes did not change and the VAF values were higher than that of subclone genes (Figure 3B). Patient 36 had a local relapse. IDH:p.R132H mutation as a driver gene in primary tumor shifted into IDH:p.R338Efs*3 mutation in the relapse sample, has been associated with substantially shorter progression-free survival(Figures 3C and 3D). To sum up, we do not see a fundamental change in driver genes during local progression of astrocytoma.

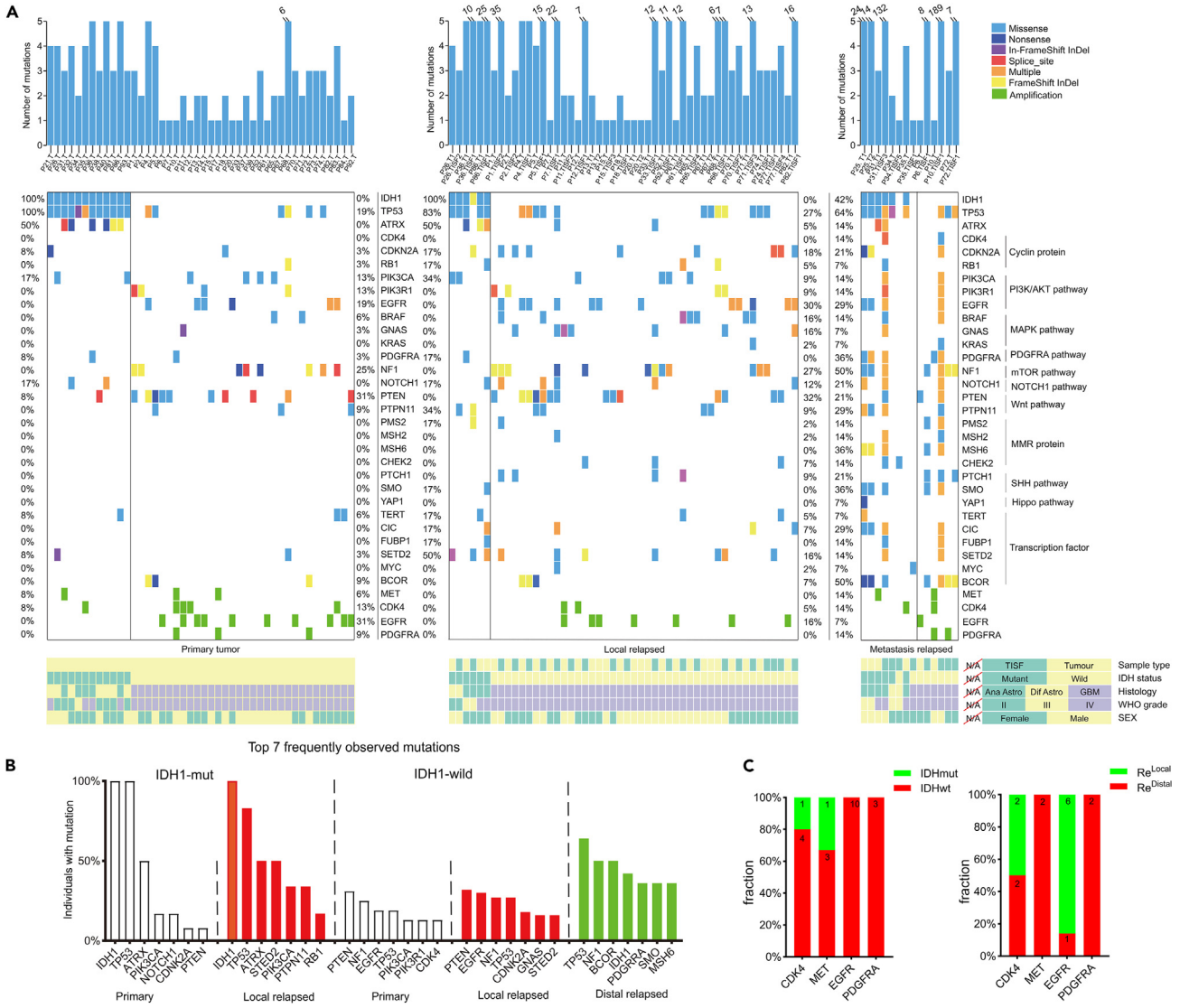

Figure 2. Longitudinal mutational landscape of gliomas

(A) Genomic profiles of primary, local relapse, and distant relapse gliomas. The number of non-synonymous mutations and mutation profiles are shown from top to bottom of the panel.

(B) Top 7 mutations in primary tumor and relapse TISF, indicating the genetic path to glioma relapse.

(C) The proportion of MET, CDK4, EGFR, and PDGFRA amplification in IDH-mutant subtype and local relapse were showed.

Patient 25 initially had been diagnosed with a lesion in the right frontal lobe in 2018, and accepted long-term TMZ treatment. Unfortunately, multiple lesions were detected by imaging in 2020, which situated in the right frontal lobe and left cerebral peduncle. Sequentially, the patient then received surgical resection for the lesion in the right frontal lobe, and the pathological diagnosis was diffuse astrocytoma (WHO grade III). IDH and TP53 mutations were identified as driver genes in tissue (Figure 3E). Meanwhile, multiple oncogenic signaling pathways, such as MMR, RAS/PDGFRA, EGFR, NOTCH1, Hedgehog, and YAP1/Hippo signaling pathways, were also be detected. These molecular features potentially increased tumor malignancy and granted them latent distant-initiating capacity for gliomas. We only detected five low-VAF mutations in the TISF1 sample, and the tumor burden progressed slowly up to Day 157. When the left cerebral peduncle lesion achieved substantial progression, the patient underwent the second surgery. Both TISF2 and TISF3 samples were obtained preoperatively and postoperatively, respectively. The pathological examinations were almost identical to that of the right frontal lesion. Further analysis revealed a large number of novel subclonal mutations appeared in the latter tissue. PDGFRA:p.V536E and CDKN2A:p. L16Pfs*9

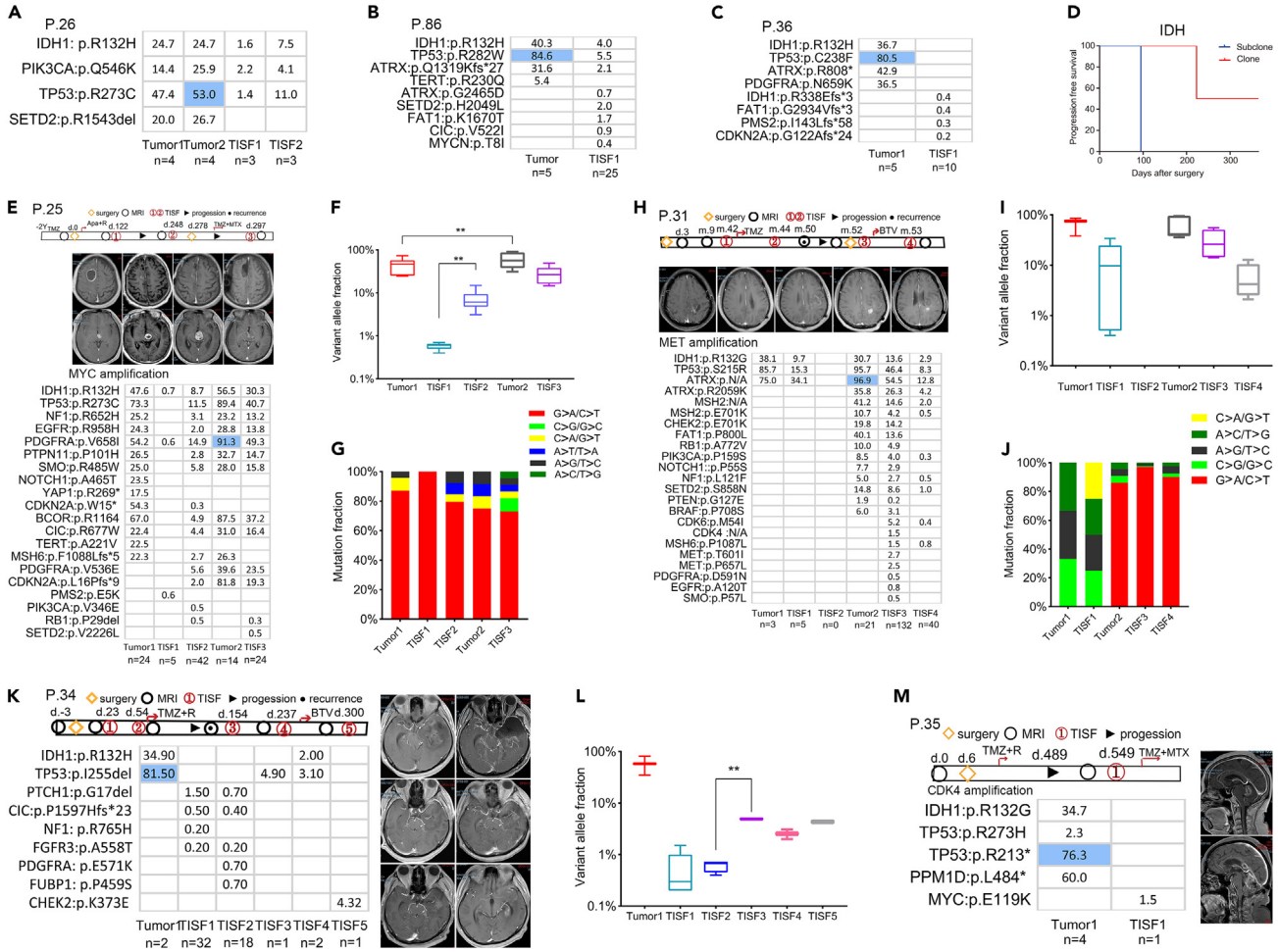

Figure 3. MMR mutations and IDH transformation promote distant relapse in IDH-mutant gliomas

(A and B) Gene evolution are showed during local relapse in Patient 26 and Patient 86.

(C and D) Gene evolution in Patient 36, with transformation of the IDH mutation site. Shorter progression-free survival compared to Patient 26 and Patient 86 during gene evolution.

(E) Clinical treatment, imaging alterations and gene evolution were shown in Patient 25.

(F) Distribution of the top five VAFs among the samples were showed. TISF2 exhibited significantly higher VAF levels than TISF1 during progression($p < 0.01$).

(G) The proportion of TMZ-associated mutations calculated in tumor and TISF samples respectively.

(H) Clinical treatment, imaging alterations and gene evolution were shown under stress treatment in Patient 31.

(I and J) Distributions of mean VAF levels and proportion of TMZ-associated mutations were shown in tumors and TISF samples.

(K) Clinical treatment, imaging alterations and gene evolution were depicted under stress treatment in Patient 34.

(L) Distribution of all mutation VAFs were revealed in tumor and TISF samples.

(M) Clinical treatment, imaging alterations and gene evolution were described in Patient 35.

mutations were identified in the TISF2 and tissue samples. The average VAF value of the top 5 mutated genes had significantly increased (Figure 3F). The acquired CDKN2A mutation progressed rapidly and was probably associated with an increase in proliferating stem-like cells.[11] Meanwhile, the tumor load increased rapidly according to imaging. We observed a characteristic change in the typical TMZ-induced mutational signature, which was associated with an increase in the proportion of C>T/G>A transversions (Figure 3G).This indicates that gliomas harbor significant heterogeneity. MMR gene mutations could facilitate acquiring additional subclone mutations during gene evolution, which may represent a novel mechanism contributing to the malignant progression of gliomas.

Patient 31 underwent initial surgical resection, and received a histopathological diagnosis of WHO grade II astrocytoma in 2014. The patient then experienced a known recurrence and accepted a second resection in

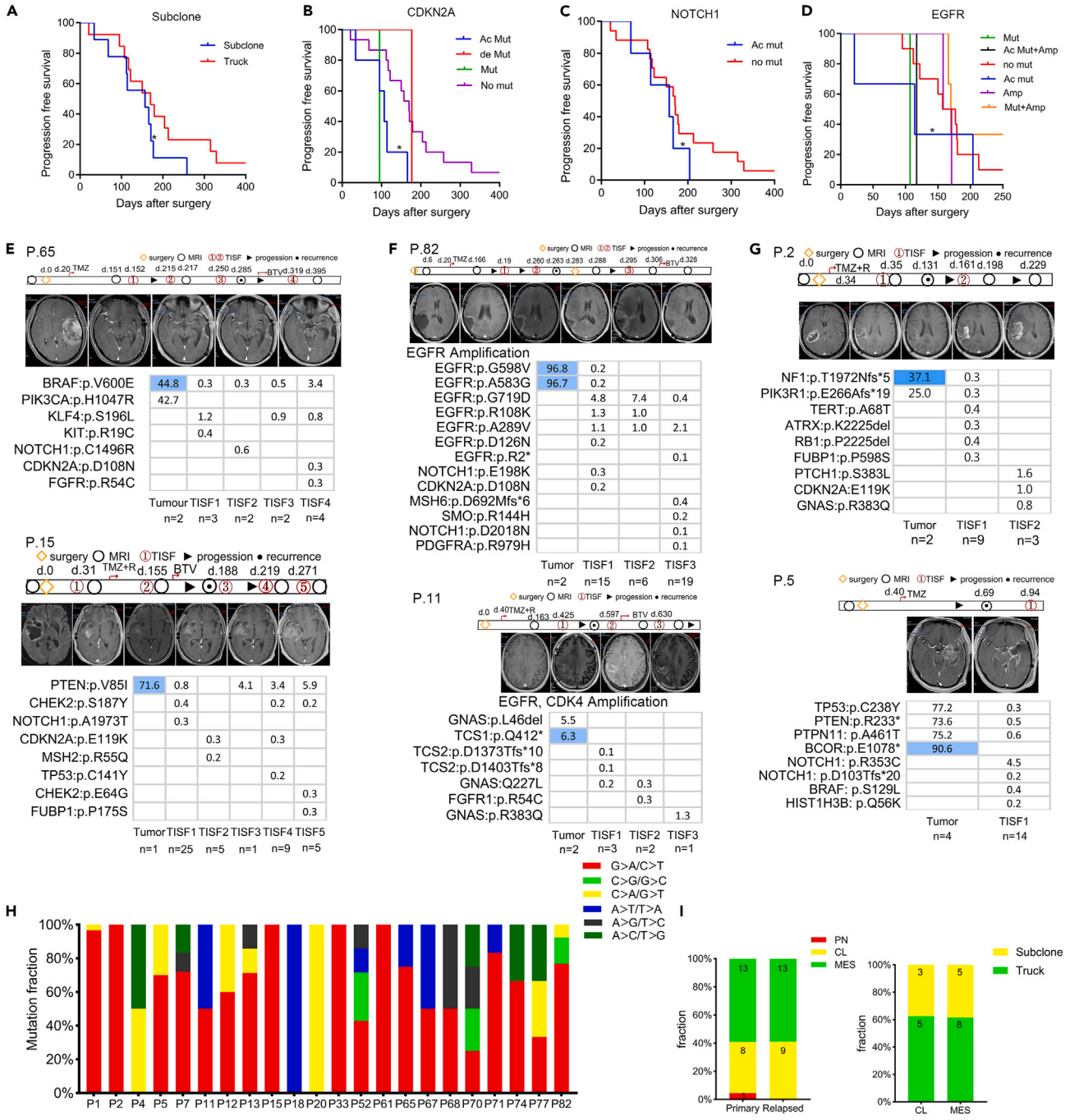

Figure 4. Genomic profiling and clonal evolution analysis of local relapse in IDHwt gliomas

(A) Significantly higher progression-free survival in trunk non-transformation compared to trunk transformation during gene evolution ($p < 0.01$).

(B–D) Shortened progression-free survival in patients with acquired EGFR, NOTCH1, and CDNK2A mutations ($p < 0.01$).

(E) Clinical treatment, imaging alterations and gene evolution were showed during local relapse progression in Patient 65 and Patient 15. Among them, and different subclone genes appeared during gene evolution.

(F) Clinical treatment, imaging alterations, and gene evolution were depicted during tumor procession in Patient 82 and Patient 11. A switch between differentially mutated patterns of the same gene occurred during gene evolution.

(G) Clinical treatment, imaging alterations, and gene evolution were described under stress treatment in Patient 2 and Patient 5. Among them, the main gene changed.

(H) Proportion of TMZ-associated mutations calculated in local relapses.

Figure 4. *Continued*

(I) The proportions of classic subtype and mesenchymal subtype in primary and local relapse were shown. The proportion of trunk gene transformation in classic and mesenchymal subtype was depicted. Ac Mut: acquired mutation; de Mut: deleted mutation; Mut: persistent mutation; No Mut: No mutation. Amp: Amplification.

2017. Gene analysis identified TP53:p.S215R, ATRX: p.N/A and IDH1:p.R132G as significantly mutated driver genes. The patient received standard chemotherapy including TMZ. Three years later, IDH, ATRX and TP53 mutant genes were detected in the TISF1 sample. Subsequently, distant relapse occurred and reoperation was performed at 52 months after the initial operation. Both TISF3 and tissue samples were collected at the same time point (Figure 3H). The average VAF value of the top 5 mutated genes significantly increased, which was followed by rapid progression (Figure 3I). Meanwhile, the case harbored multiple subclonal mutations in the relapse tissue and sample, including NF1, NOTCH1, PTEN, RB1, BRAF and FAT1, accompanied by MSH2:p.N/A and MSH2:p.E701K mutations with a VAF of 41.2% and 10.7%, respectively. Similarly, we observed hypermutation in TISF3 samples. EGFR, PDGFRA and SHh singling pathways were also activated in addition to the above mutations. MMR mutations may contribute to TMZ resistance and relapse.[22,23] A typical TMZ-induced mutational signature associated with an increase in the proportion of C>T/G>A transversions was observed (Figure 3J). The genetic alterations associated with distant relapse demonstrated greater heterogeneity. TMZ-induced genomic characteristics were substantially associated with invasiveness. These results indicate that distant relapse represents a late event in astrocytoma during evolution under therapy.

Low-grade gliomas (LGGs) grow slowly but mostly eventually progress to high-grade gliomas. Patient 34 underwent surgical resection and received a diagnosis of astrocytoma (WHO grade III) in 2020. TP53:p.I255del and IDH1:p.R132H mutations were identified as early driver events. Further analysis found that several subclonal mutations with low VAF values appeared in the TISF1 samples. Only the TP53:p.I255del mutation with a VAF of 4.9% in the TISF3 sample could be observed, which was followed by tumor local progression at 6 months after the operation. Distant relapse occurred under treatment, and a novel subclonal mutation CHEK2:p.K373E with a VAF of 4.32% was detected in the TISF5 sample. However, IDH1 and TP53 mutations disappeared. Here, we demonstrated that the IDH-mutant type likely shifted to a more aggressive gene phenotype (Figures 3K and L). Patient 35 harbored TP53:p. R213*, PPM1D:p.L484* and IDH1:p.R132H as driver mutations (WHO grade IV). Distant relapse occurred at 18 months after operation, and only a subclone mutation MYC:p. E119K was detected with a VAF of 1.5% in the TISF sample (Figure 3M). Changes in IDH mutations indicated that the cell phenotype will also shift during tumor evolution, progressed to higher malignancy grades, which likely represented another primary gene evolution pattern in astrocytoma.

Genomic profiling and clonal evolution analysis of local recurrence IDHwt glioma

Glioblastomas exhibit significant heterogeneity during gene evolution. Our study reveals a highly branched evolutionary pattern, with 41% (9/22) of patients experiencing changes in trunk genes. This behavior likely facilitates tumor progression (Figures 4A and 4I). Our findings suggest that the RAS (EGFR, GNAS, BRAF) and NOTCH1 signaling pathways, along with the cycle protein (CDKN2A), play a crucial role in local progression. The progression-free survival of patients who acquired a CDNK2A mutation during gene evolution was notably shortened(Figure 4B). We observed similar results with acquired EGFR and NOTCH1 mutations (Figures 4C and 4D). We hypothesize that subclone gene reconstruction, occurring during tumor evolution, likely plays a significant role in tumor progression and drug resistance.

Patient 65 underwent surgical resection and had a pathological diagnosis of glioblastoma (WHO grade IV). Two driver mutations, BRAF:p.V600E and PIK3CA: p.H1047R, were detected in tumor tissue. Under radiotherapy and TMZ treatment, further analysis revealed the appearance of subclonal mutations with low VAF values during gene evolution. These mutations, KLF4:p.S196L, NOTCH1:p.C1496R and CDNK2A:p.D108N mutations, appeared successively. As local relapse progressed, the driver gene BRAF:p.V600E remained unchanged with a VAF of 3.4% in the TISF4 (Figure 4E). Patient 15 underwent surgery and harbored a driver mutation, PTEN: p.V85I. Under TMZ treatment, NOTCH1:p.1973T and CDNK2A:p.E119K appeared successively. Recurrence was observed on imaging after seven months. The driver gene PTEN:p.V85I mutation, with a VAF of 4.1%, remained unchanged in the TISF3. The patient then received TMZ and Bev treatment. Further analysis revealed the appearance of some subclonal mutations, TP53:p.C141Y and CHEK2:p.E64G, with low VAF values during gene evolution (Figure 4E). The results suggest that although the main gene

remained unchanged during tumor evolution, subclonal mutations appeared, potentially contributing to treatment resistance.

A switch between differentially mutated versions of the same gene also occurred in EGFR and GNAS. Patient 82 underwent surgery and received a histological diagnosis of glioblastoma (WHO grade IV). EGFR:p.G598V and EGFR:p.A583G mutations were detected as driver genes, and EGFR gene amplification were also observed. EGFR: p.G598V mutation is a common activating mutation in glioblastoma, which increases EGFR autophosphorylation levels.[24] EGFR:p.G719D and EGFR:p. A289V were soon observed in TISF1 and TISF2 samples during the progression of evolution. EGFR:p.G719D converted to a trunk gene, and the VAF level also increased from 4.8% to 7.4%. One month after reoperation, the tumor continued to progress. EGFR:p.A289V mutation, with high VAF in TISF3 sample, shifted into a trunk gene. EGFR:p.A289V presents a more invasive and aggressive phenotype.[25] A case was Patient 11. GNAS:p.L46del was present as a driver gene in the initial tumor sample. GNAS:Q227L, with low VAF, was found in TISF1 and TISF2 samples. GNAS:Q227L often leads to continuous activation of G protein-coupled signal pathway,[26] which plays a crucial role in tumor progression. The patient subsequently received Bev treatment after recurrence. The trunk gene converted to GNAS:p.R383Q, which may be associated with Bev resistance (Figure 4F). These clonal switching events within the same gene occurred preferentially in genes known to play a significant role in glioma progression. The switching of key driver genes suggests that convergent evolution contributes to late expansion and therapy resistance.

In total, we discovered that 42% (9/22) of patients with locally recurrent GBM experienced clonal replacements in key driver genes. Patient 5, who underwent surgery and was pathologically diagnosed with glioblastoma, received TMZ treatment. Relapsed was soon observed on imaging after three months. The trunk genes shifted from TP53:p. C238Y and PTEN:p.R233* to NOTCH1:p.R353C mutation, indicating a more highly invasive phenotype. Patient 2 underwent surgery and received a pathological diagnosis of glioblastoma in 2020, WHO grade IV. NF1:p.T1972Nfs*5 and PIK3R1:p.E266Afs*19, identified as driver genes, were detected. Recurrence was soon observed on imaging after six months under treatment. As local relapse occurred, some subclonal mutations, PTCH1:p.S383L and CDKN2A:p.E119K, were detected with a VAF of 1.6% and 1.0% in the TISF2 sample (Figure 4G). It appears that the transformation of trunk genes promotes tumor progression during gene evolution, likely representing another primary evolutionary pattern. In patients with local relapse, the proportion of C>T/G>A transitions did not significantly increase (Figure 4H). While classic subtype and mesenchymal subtype are the main types in patients with local relapse (Figure 4I). In this study, we demonstrated the three main gene evolution patterns, including subclonal reconstruction, trunk gene transformation and convergent evolution. Our genomic studies have shown that gene evolution can promote tumor recurrence and the development of therapy-resistant tumor cell populations (Figure S1 shows mutational gene landscape during evolution).

PDGFRA and SHh signaling pathways promote distant relapse in IDHwt glioma

Nearly all glioblastomas progress or recur, both locally (~80%) and distally (~20%).[7] To elucidate the relationship between biological characteristics and gene evolution, we examined three cases of distant recurrent glioblastoma. These cases showed mutational profiles enriched in the PDGFRA and SHh signaling pathways. One case, with PDGFRA:p.E997Q and PDGFRA amplification, acquired significantly more mutations (>100) during the progression of gene evolution, This case harbored mutations in DNA mismatch repair genes (MSH6 and PMS2), consistent with a hypermutation genotype. The most frequent mutations were C>T/G>A transitions (Figures 5A–5C). More subclones emerged, indicating a more highly invasive phenotype during distant relapse progression.

Patient 72, with a cerebellar lesion, underwent surgery and received a histopathological diagnosis of GBM (WHO grades IV). NF1:p.A211Sfs*4, TP53: p.R158G, and PDGFRA amplification were identified as driver genes. Distant relapse was soon observed on imaging after eight months (Figure 5D). TP53 inactivation and NF1 mutation play a synergistic role in the occurrence and development of human malignant astrocytoma.[27] The above two patients were classified based on their molecular subtype into PN. The mesenchymal (MES) subtype was most stable (65%), while the classical (CL, 51%) and PN (41%) subtypes were less frequently retained.[28] PN-to-MES switching has been related to treatment resistance in GBM relapse.[29] This switching tends to increase the degree of malignancy and results in phenotypic shifts. Patient 5 underwent surgery and had a pathological diagnosis of glioblastoma, WHO grade IV. PTEN: p.Y27C mutation and EGFR amplification were detected in the initial tumor. Distant relapse was soon observed on

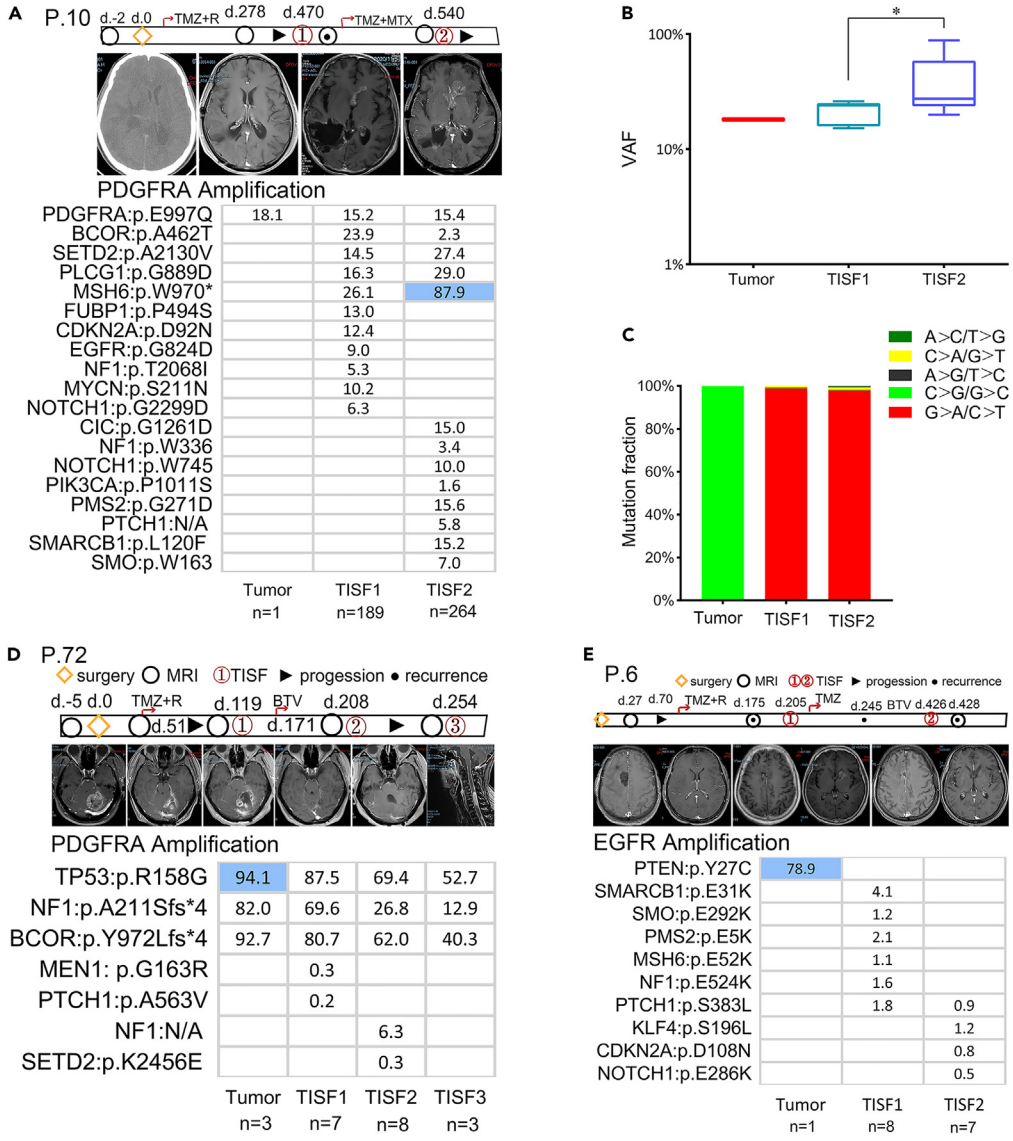

Figure 5. PDGFRA and SHh singling pathways promote distant relapse in IDHwt gliomas

(A) Clinical treatment, imaging alterations and the time of ctDNA extraction were shown during tumor progression in Patient 10. Hypermutation occurred in TISF1 detection 470 days after operation under the TMZ treatment.

(B) Significant variation in VAF, with higher average top five VAF values in TISF2 compared to TISF1 during the progression period ($p < 0.01$).

(C) Proportion of TMZ-associated mutations calculated in tumor and TISF samples.

(D and E) Clinical treatment, imaging alterations, and genomic profiles were depicted during tumor relapse in Patient 72 and Patient 6.

imaging after five months. SHh (SMO:p. E272K, SMARCB1:p.E31K) signaling and NF1 mutations were detected as the trunk genes.[30] The patient subsequently received Bevacizumab (Bev), and the distant relapse lesion significantly disappeared. The trunk genes converted into KLF4:p.S196L and CDKN2A:p.D108N (Figure 5E). Previous studies suggested that SHh signaling accounts for the initiation and maintenance of tumor growth, as well as for drug resistance and distant relapse. It also regulates self-renewal of highly malignant cancer stem cells.[31] Glioblastoma exhibits great heterogeneity during evolution. The PN subtype is dominated by stem-like cells and has poor stability. Therefore, it is prone to change subtypes and acquire subclone genes during gene evolution, such as MMR, SHh signaling, NF1 and TP53 co-mutations, promoting malignant progression and distant relapse.

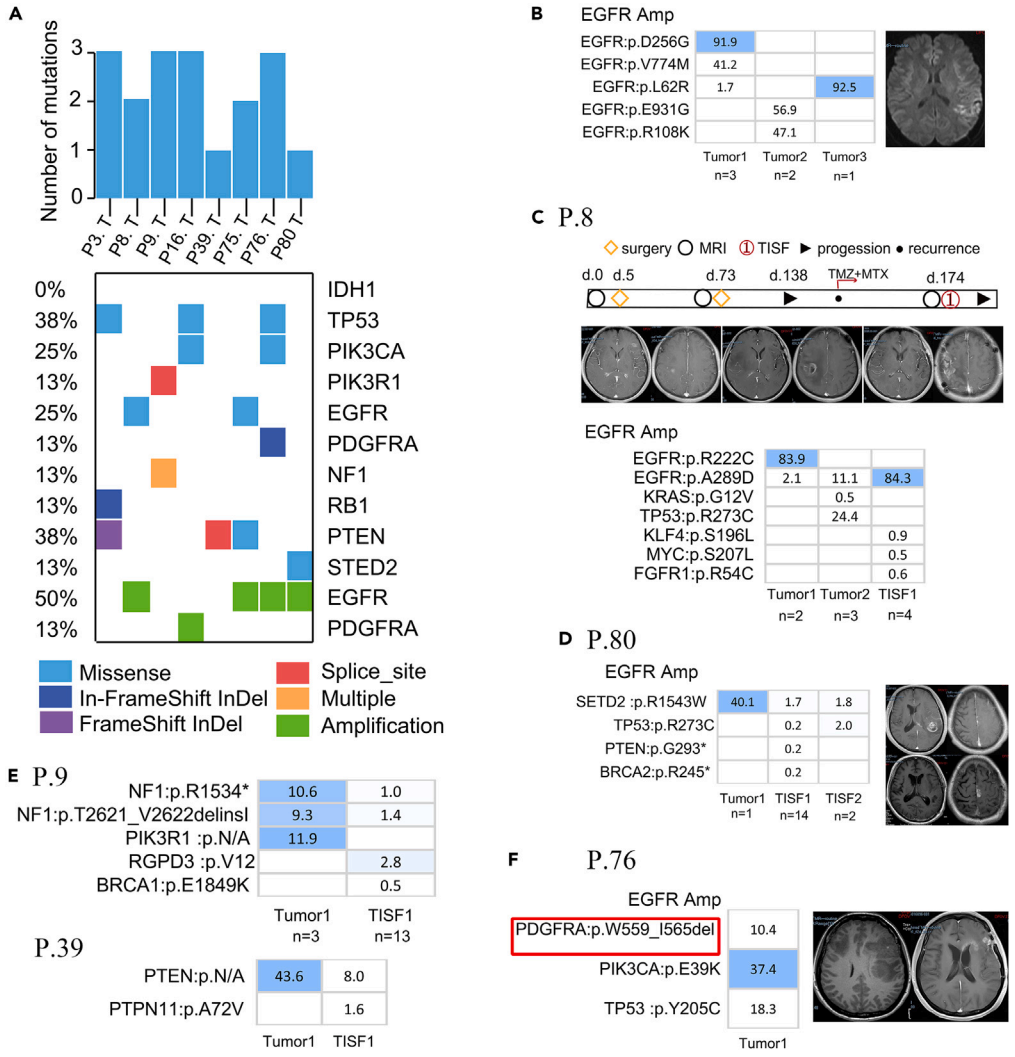

Figure 6. Genetic evolution of multifocal glioma

(A) Summary of genomic profiles of multifocal gliomas.

(B) Genomic profiles of three sites from one lesion in patient 70.

(C) Clinical treatment, imaging alterations and the time of ctDNA extraction were depicted in patient 8. Gene profiles in tumor and TISF samples were shown.

(D) Clinical treatment and imaging alterations in patient 80 were depicted. Gene profiles in tumor and TISF samples were described.

(E) Gene profiles when other lesion progressed was shown in patient 9 and patient 39.

(F) Gene profiles and imaging alterations in patient 76 were depicted.

Genetic evolution of multifocal glioma

There are two possible explanations for the development of multifocal gliomas (multiple synchronous lesions in one patient): (1) detaching the tumor cells from the primary glioma and migrating to other site at a later stage of tumor or (2) parallel evolution of gliomas from a common precursor clone with subsequent subclonal reconstruction. Our results suggest that the latter scenario is more likely. Genetic studies on multifocal gliomas are very rare. In our study, among 8 multifocal gliomas, all were IDH wild-type glioblastomas. We also recently identified that the CL subtype (4/8) had a substantially higher proportion of patients with multifocal gliomas (Figure 6A). Glioblastoma exhibits great heterogeneity, not only in the diversity of cell subtypes, but also in gene mutations. Patient 70, with a parietal lesion, underwent surgery and received a histopathological diagnosis of GBM (WHO grades IV). We harvested tumor cells from three different sites and observed significant differences in mutation spectra. EGFR:p.D256G, EGFR:p.E931G

and EGFR: p.L62R were detected respectively, and all accompanied by EGFR amplification (Figure 6B). Patient 8 was initially diagnosed multiple lesions by imaging in 2019, located in the left frontal lobe and in the right parietal lobe. After surgically resecting the lesion in the left frontal lobe, the histopathological diagnosis of the lesion was GBM. We confirmed EGFR:p.R222C and EGFR:p.A289D mutations with VAF levels of 83.9% and 2.1% respectively, accompanying EGFR amplification in the tumor sample. 67 days after diagnosis, the patient underwent a second surgical resection when the right parietal lesion showed significant progression. We confirmed TP53:p.R273C and EGFR:p.A289D mutations with VAF values were 24.1% and 11.1% respectively, accompanying EGFR amplification. The right parietal lesion showed significant progression after two months. EGFR:p.A289D mutation with a VAF of 84.3% was detected in the TISF sample(Figure 6C). Both lesions have EGFR gene amplification, but the subclonal genes are significantly different. Therefore, we believe that multifocal gliomas may originate from a monoclonal gene.

Patient 80 was initially diagnosed with multiple lesions in the left frontal and left parietal lobe, then underwent parietal lesion resection. EGFR amplification and STED2:p.R1543W mutation were confirmed as driver genes. The left frontal lesion showed significant progression. Another emerging driver gene, TP53:p.R273C, appeared, accompanying EGFR amplification and STED2:p.R1543W mutation in TISF sample (Figure 6D). Patient 9 was initially diagnosed with multiple lesions in the left temporal and parietal lobes and underwent resection. NF1:p.R1534* mutation and NF1:p.T2621-V2622delinsl were detected. Multiple lesions showed significant progression. RGPD3:p.V12L mutation was detected, accompanying by NF1 mutation in the TISF sample. Patient 39 was initially diagnosed with multiple lesions in the left temporal lobe. We confirmed PTEN: p.N/A as a driver gene. Multiple lesions progressed rapidly. A novel gene mutation, PTPN11:p.A72V, emerged, while the driver gene remained unchanged (Figure 6E). PTPN11:p.A72V has been shown to activate protein tyrosine phosphatases.[32] These main driver mutations of multifocal gliomas are consistent. We consistently found additional subclonal genes that differed between foci from the same patient. This suggests that multifocal glioma may originate from a monoclonal gene in different sites, undergo parallel evolution, and exhibit significant heterogeneity.

Patient 76 was initially diagnosed with multiple lesions in the right frontal and left parietal lobe. TP53:p.Y205C and PIK3CA:p.E39K was detected in the initial tumor, accompanied by EGFR amplification and PDGFRA:p.W559_I565del mutation. Distant relapse occurred in the process of evolution (Figure 6F). Another lesion, located contralaterally and close to the ventricular wall, may suggest CSF dissemination. PDGFRA may have played an important role in distant relapse. Multifocal gliomas undergo parallel evolution and may be similar to that of a single lesion.

Tracking the distant relapse cascade of glioma

There were significant differences in the gene evolution of the IDH-mutant and IDH wild-type gliomas under therapy. Our studies showed that IDH-mutant gliomas primarily evolve in two major ways: (1) After long-term TMZ chemotherapy, MMR gene mutations appeared, leading to an accumulation of gene mutations and activation of specific signaling pathways, such as PI3K/AKT (EGFR, PIK3CA), NOTCH1, Wnt (PTEN), SHh (SMO), and RAS (PDGFRA). This results in increased malignancy of the tumor and distant recurrence; or (2) under long-term stress treatment, we observed IDHmut-to-IDHwt transformations in our cases. These transformations shift into higher grades and tend to progress rapidly, indicating that the cell phenotype and genetic characteristics can change during the process of glioma evolution. Distant relapse may be a later event in IDH-mutant gliomas under therapy (Figure 7A).

Among IDH-wildtype glioblastomas, different subtypes also exhibited their own preferred patterns of evolution under stress treatment: (I)The MES and CL subtypes are relatively stable, However, they also exhibit great heterogeneity, largely affected by the process of gene evolution. We propose three main evolution patterns accounting for local relapse: trunk genes transformation, subclone reconstruction and and convergent evolution. or (II) PN subtype gliomas, accompanied by PDGFRA gene amplification, are prone to hypermutation and PN-to-MES switching. The degree of tumor malignancy and the probability of distant relapse significantly increase (Figure 7B). Therefore, gliomas have their own preferred evolution patterns.

DISCUSSION

In our study, we found clear biological distinctions and differences in the evolution cascade of gliomas using liquid biopsy analytes. However, the ultimate goal must be clinical decision-making. It is technically and humanly feasible to monitor cancer progression in real-time for glioma patients, Liquid biopsy

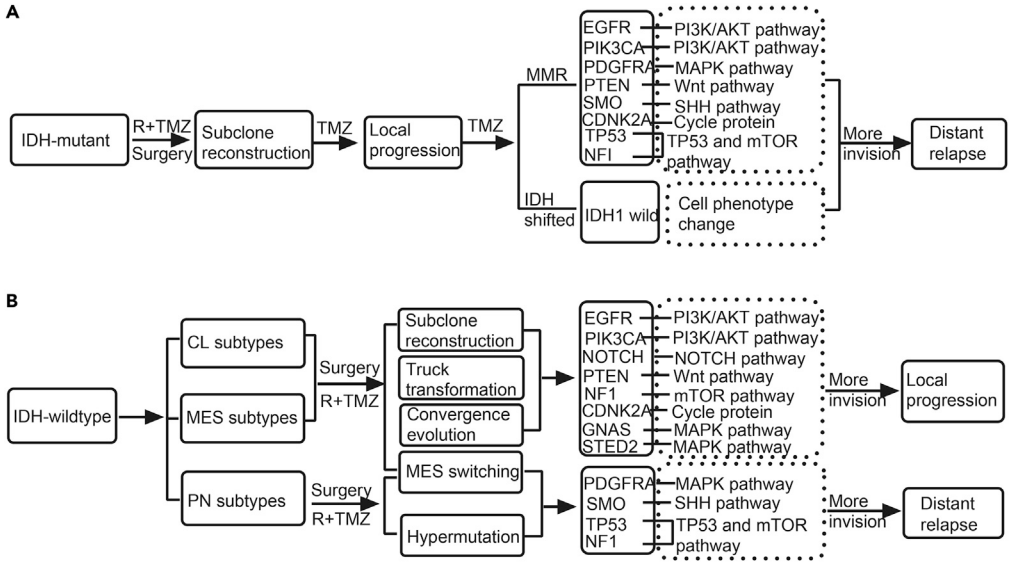

Figure 7. Tracking the distant relapse cascade of glioma patients

(A) General evolution trajectory of distant relapse was depicted under pressure therapy in IDH-mutant glioma.

(B) General path of evolution in IDH wild-type gliomas was showed under stress therapy.

(TISF-ctDNA) holds the promise of becoming a minimally invasive tool for molecular profiling and relapse monitoring in glioma patients.

Previous studies have identified three distinct relapse-specific phenotypes: neuronal, mesenchymal, and proliferative. IDH-mutant and PN gliomas primarily consist of proliferating stem-like and stem-like neoplastic cells. Hypermutation is also associated with increased proliferating stem-like neoplastic cells.[11] Therefore, hypermutation is more likely to occur in IDH-mutant and PN subtype gliomas. Our study identified two cases of hypermutation in these subtypes. Somatic mutations in DNA mismatch repair genes have been associated with a hypermutated phenotype. Multiple signaling pathways are activated may explain why hypermutations are thought to facilitate distant relapse during tumor evolution. In this study, we observed marked aggressive progression through IDH-mutant transformation. This indicates that the cell phenotype and genetic characteristics of IDH-mutant gliomas can change during tumor evolution. It is clear that IDHmut-to-IDHwt transformation is also a malignant shift during tumor evolution, likely prone to distant relapse.

The CL and MES subtypes were dominated by differentiated-like neoplastic cells. Stem-like neoplastic cells of these tumors increase infiltration into the brain parenchyma at the invasive margin. Genes related to neuronal signaling are upregulated at relapse.[11,33] Our study demonstrates that CL and MES subtype gliomas have a higher propensity for local relapse. We observed three evolution patterns, including subclone gene reconstruction, trunk gene transformation, and convergence evolution, which contribute to promoting tumor progression and exerting drug resistance. Genomic alterations in the mutated genes (e.g., CDNK2A and GNAS) and altered pathways (e.g., EGFR and NOTCH1) occur significantly more frequently. Furthermore, patients with acquired CDKN2A mutation progress rapidly locally, prone to a rapidly local progressive course. The perivascular niche (PVN) within the GBM tumor microenvironment contributes to tumor cell invasion and stem cell maintenance. EGFR, PI3K/Akt and Ras/MAPK signaling pathways are activated in the PVN model.[34] Previous work has also demonstrated that NOTCH signaling acts as a central switch between the PVN and network niche in glioma.[35] NOTCH signaling induces GSC invasion along white matter tracts.[36] In our study, NOTCH signaling was significantly associated with a higher risk of local recurrence in the CL and MES subtypes. Similarly, our studies suggest that genomic alterations in EGFR and RAS signaling pathways are also more frequent during gene evolution. In summary, The CL and MES subtypes are more prone to local progression through gene evolution.

In IDH-wildtype gliomas, non-hypermutated relapse that acquired NF1 mutation undergo a mesenchymal transition and show an increase in granulocytes and myeloid cells.[11] Longitudinally, IDHwt gliomas

undergoing a mesenchymal transition during invasion exhibited myeloid-specific expression profiles at relapse. The mesenchymal transition endowed the classical and PN subtypes with multiple biological characteristics, formed highly aggressive tumors. We identified that the activation of SHh signaling and co-mutation of TP53 and NF1 appeared during the mesenchymal transition, and which promotes distant relapse. Previous work suggested that SHh signaling is an important and substantial regulator of VEGF and NOTCH pathways.[37] Co-mutation of TP53 and NF1 play a synergistic role in the promotion of malignant progression.[27] We concluded that subclone reconstruction occured during the mesenchymal transition, which has achieved the biological characteristics of distant relapse. Distant relapse in glioma can be a late event during tumor progression.[38]

Mathematical modeling delineated the sequential order of somatic mutational events that constitute GBM genome architecture, identifying somatic mutations in IDH1, PIK3CA, and ATRX as early events, whereas PTEN, NF1, and EGFR alterations were predicted to occur at a later stage of the evolution.[39] Kim et al. analyzed the TCGA dataset to identify clonal (early) and subclonal (late) events by integrating variant allele fractions and concluded that alterations in TP53 and PIK3CA/PIK3R1 were likely founder events, while EGFR, PDGFRA, and PTEN alterations could occur at different time points.[40] However, our results showed that the alterations that were always shared between foci in one patient—and therefore might be early founder events—were PTEN mutation and EGFR amplification. Common events are not necessarily early events in glioblastoma genesis but rather could have occurred later. Multifocal gliomas do not have the gene characteristics of distant relapse mentioned above. Multifocal gliomas likely originated from ordinary tumor precursor cells in different sites and demonstrated parallel evolution.

Our work has highlighted heterogeneity during tumor evolution consistent with previous studies.[41,42] The monitoring of ctDNA has been used to assess treatment response and to detect early relapse after surgery.[43,44] These striking differences in gene evolution and biological characteristics of different glioma subtypes have significant clinical implications for decision-making. Overall, our results demonstrate that different subtypes of glioma exhibit distinct models of preferential evolution under stress treatment, providing a basis for establishing a prediction model of evolution. We have reported for the first time the real-time evolution of gliomas *in vivo* under the stress treatment. Our research shows that different subtype gliomas have their own preferred evolution patterns under stress treatment, providing a foundation for establishing a prediction model of evolution. Future efforts of the GLASS consortium include expanding the cohort, integrating digital tissue sections, and associating clinical and genomic datasets with radiographic imaging data.[45] Further research strategies should focus on the future efforts of the GLASS consortium.

Limitation of the study

Given the limitations of exome sequencing, we acknowledge the obvious disadvantages of this analysis. It is likely that we were unable to elaborate on evolution information for some important driver events, such as TERT promoter mutation and MGMT promoter methylation. Due to the limitation of sample size, we only described the gene evolution about local recurrence and distant recurrence. With the increase of our samples, we will further elaborate gene evolution of different subtypes. Further research strategies should focus on the disadvantages described above.

STAR★METHODS

Detailed methods are provided in the online version of this paper and include the following:

- KEY RESOURCES TABLE
- RESOURCE AVAILABILITY
  - Lead contact
  - Materials availability
  - Data and code availability
- EXPERIMENTAL MODEL AND SUBJECT PARTICIPANT DETAILS
  - Patient characteristics
  - Samples collection
- METHOD DETAILS
  - DNA extraction
  - ctDNA sequencing

- QUANTIFICATION AND STATISTICAL ANALYSIS
  - Mean mutant molecules per milliliter (mMMPM)
  - Statistical analysis

SUPPLEMENTAL INFORMATION

Supplemental information can be found online at https://doi.org/10.1016/j.isci.2023.107528.

ACKNOWLEDGMENTS

We thank Professor Juha Hernesniemi for his help and advice in the process.

Funding: The research was supported by the Henan Province Science and Technology Tackle Program (No.192102310126), the Joint Project of Medical Science and Technology Tackling Plan of Henan Province (No.201601016), and the Henan Medical Science and Technology Research Youth Co-construction Project(No. SJGJ202103017).

AUTHOR CONTRIBUTIONS

Conception and design, X.B. and M.L.; the inpatient's treatment and sample acquisition, G.L., C.B., G.G., Z.Z., and Y.G.; analysis and interpretation of data, G.L., Z.S., K.D., and S.W.; acquisition of data, X.S. and Y.B.; histopathological examination, G.L. and L.K.; imaging examination, M.W.; administrative, technical, or material support, T.L.; writing, review, and/or revision of the manuscript, all authors; All authors read and approved the final manuscript.

DECLARATION OF INTERESTS

The authors declare that they have no competing interests.

Received: October 6, 2022
Revised: June 18, 2023
Accepted: July 28, 2023
Published: August 2, 2023

REFERENCES

1. Williams, M.J., Werner, B., Heide, T., Curtis, C., Barnes, C.P., Sottoriva, A., and Graham, T.A. (2018). Quantification of subclonal selection in cancer from bulk sequencing data. Nat. Genet. *50*, 895–903. https://doi.org/10.1038/s41588-018-0128-6.

2. Pantel, K., and Alix-Panabières, C. (2019). Liquid biopsy and minimal residual disease - latest advances and implications for cure. Nat. Rev. Clin. Oncol. *16*, 409–424. https://doi.org/10.1038/s41571-019-0187-3.

3. (2020). MRD May Predict Relapse in NSCLC. Cancer Discov. *10*, OF7. https://doi.org/10.1158/2159-8290.CD-ND2020-010.

4. Ignatiadis, M., Sledge, G.W., and Jeffrey, S.S. (2021). Liquid biopsy enters the clinic - implementation issues and future challenges. Nat. Rev. Clin. Oncol. *18*, 297–312. https://doi.org/10.1038/s41571-020-00457-x.

5. Nong, J., Gong, Y., Guan, Y., Yi, X., Yi, Y., Chang, L., Yang, L., Lv, J., Guo, Z., Jia, H., et al. (2018). Circulating tumor DNA analysis depicts subclonal architecture and genomic evolution of small cell lung cancer. Nat. Commun. *9*, 3114. https://doi.org/10.1038/s41467-018-05327-w.

6. Fribbens, C., Garcia Murillas, I., Beaney, M., Hrebien, S., O'Leary, B., Kilburn, L., Howarth, K., Epstein, M., Green, E., Rosenfeld, N., et al. (2018). Tracking evolution of aromatase inhibitor resistance with circulating tumour DNA analysis in metastatic breast cancer. Ann. Oncol. *29*, 145–153. https://doi.org/10.1093/annonc/mdx483.

7. Spiteri, I., Caravagna, G., Cresswell, G.D., Vatsiou, A., Nichol, D., Acar, A., Ermini, L., Chkhaidze, K., Werner, B., Mair, R., et al. (2019). Evolutionary dynamics of residual disease in human glioblastoma. Ann. Oncol. *30*, 456–463. https://doi.org/10.1093/annonc/mdy506.

8. Choi, S., Yu, Y., Grimmer, M.R., Wahl, M., Chang, S.M., and Costello, J.F. (2018). Temozolomide-associated hypermutation in gliomas. Neuro Oncol. *20*, 1300–1309. https://doi.org/10.1093/neuonc/noy016.

9. Yu, Y., Villanueva-Meyer, J., Grimmer, M.R., Hilz, S., Solomon, D.A., Choi, S., Wahl, M., Mazor, T., Hong, C., Shai, A., et al. (2021). Temozolomide-induced hypermutation is associated with distant recurrence and reduced survival after high-grade transformation of low-grade IDH-mutant gliomas. Neuro Oncol. *23*, 1872–1884. https://doi.org/10.1093/neuonc/noab081.

10. Korber, V., Yang, J., Barah, P., Wu, Y., Stichel, D., Gu, Z., Fletcher, M.N.C., Jones, D., Hentschel, B., Lamszus, K., et al. (2019). Evolutionary Trajectories of IDH(WT) Glioblastomas Reveal a Common Path of Early Tumorigenesis Instigated Years ahead of Initial Diagnosis. Cancer Cell *35*, 692–704.e12. https://doi.org/10.1016/j.ccell.2019.02.007.

11. Varn, F.S., Johnson, K.C., Martinek, J., Huse, J.T., Nasrallah, M.P., Wesseling, P., Cooper, L.A.D., Malta, T.M., Wade, T.E., Sabedot, T.S., et al. (2022). Glioma progression is shaped by genetic evolution and microenvironment interactions. Cell *185*, 2184–2199.e16. https://doi.org/10.1016/j.cell.2022.04.038.

12. Sareen, H., Garrett, C., Lynch, D., Powter, B., Brungs, D., Cooper, A., Po, J., Koh, E.S., Vessey, J.Y., McKechnie, S., et al. (2020). The Role of Liquid Biopsies in Detecting Molecular Tumor Biomarkers in Brain Cancer Patients. Cancers *12*, 1831. https://doi.org/10.3390/cancers12071831.

13. Miller, A.M., Shah, R.H., Pentsova, E.I., Pourmaleki, M., Briggs, S., Distefano, N., Zheng, Y., Skakodub, A., Mehta, S.A., Campos, C., et al. (2019). Tracking tumour evolution in glioma through liquid biopsies of cerebrospinal fluid. Nature *565*, 654–658. https://doi.org/10.1038/s41586-019-0882-3.

14. Yu, J., Sheng, Z., Wu, S., Gao, Y., Yan, Z., Bu, C., Gu, J., Bu, Y., Deng, K., Xu, S., et al. (2021). Tumor DNA From Tumor In Situ Fluid Reveals Mutation Landscape of Minimal Residual Disease After Glioma Surgery and Risk of Early Recurrence. Front. Oncol. *11*, 742037. https://doi.org/10.3389/fonc.2021.742037.

15. Frattini, V., Trifonov, V., Chan, J.M., Castano, A., Lia, M., Abate, F., Keir, S.T., Ji, A.X., Zoppoli, P., Niola, F., et al. (2013). The integrated landscape of driver genomic alterations in glioblastoma. Nat. Genet. *45*, 1141–1149. https://doi.org/10.1038/ng.2734.

16. Biavasco, R., Lettera, E., Giannetti, K., Gilioli, D., Beretta, S., Conti, A., Scala, S., Cesana, D., Gallina, P., Norelli, M., et al. (2021). Oncogene-induced senescence in hematopoietic progenitors features myeloid restricted hematopoiesis, chronic inflammation and histiocytosis. Nat. Commun. *12*, 4559. https://doi.org/10.1038/s41467-021-24876-1.

17. McCord, M., Steffens, A., Javier, R., Kam, K.L., McCortney, K., and Horbinski, C. (2020). The efficacy of DNA mismatch repair enzyme immunohistochemistry as a screening test for hypermutated gliomas. Acta Neuropathol. Commun. *8*, 15. https://doi.org/10.1186/s40478-020-0892-2.

18. Wang, J., Cazzato, E., Ladewig, E., Frattini, V., Rosenbloom, D.I.S., Zairis, S., Abate, F., Liu, Z., Elliott, O., Shin, Y.J., et al. (2016). Clonal evolution of glioblastoma under therapy. Nat. Genet. *48*, 768–776. https://doi.org/10.1038/ng.3590.

19. Lee, D.H., Lee, S.Y., and Oh, S.C. (2017). Hedgehog signaling pathway as a potential target in the treatment of advanced gastric cancer. Tumour Biol. *39*. 1010428317692266. https://doi.org/10.1177/1010428317692266.

20. Szczepny, A., Rogers, S., Jayasekara, W.S.N., Park, K., McCloy, R.A., Cochrane, C.R., Ganju, V., Cooper, W.A., Sage, J., Peacock, C.D., et al. (2017). The role of canonical and non-canonical Hedgehog signaling in tumor progression in a mouse model of small cell lung cancer. Oncogene *36*, 5544–5550. https://doi.org/10.1038/onc.2017.173.

21. Ishaque, N., Abba, M.L., Hauser, C., Patil, N., Paramasivam, N., Huebschmann, D., Leupold, J.H., Balasubramanian, G.P., Kleinheinz, K., Toprak, U.H., et al. (2018). Whole genome sequencing puts forward hypotheses on metastasis evolution and therapy in colorectal cancer. Nat. Commun. *9*, 4782. https://doi.org/10.1038/s41467-018-07041-z.

22. Aasland, D., Götzinger, L., Hauck, L., Berte, N., Meyer, J., Effenberger, M., Schneider, S., Reuber, E.E., Roos, W.P., Tomicic, M.T., et al. (2019). Temozolomide Induces Senescence and Repression of DNA Repair Pathways in Glioblastoma Cells via Activation of ATR-CHK1, p21, and NF-kappaB. Cancer Res. *79*, 99–113. https://doi.org/10.1158/0008-5472.CAN-18-1733.

23. Cahill, D.P., Levine, K.K., Betensky, R.A., Codd, P.J., Romany, C.A., Reavie, L.B., Batchelor, T.T., Futreal, P.A., Stratton, M.R., Curry, W.T., et al. (2007). Loss of the mismatch repair protein MSH6 in human glioblastomas is associated with tumor progression during temozolomide treatment. Clin. Cancer Res. *13*, 2038–2045. https://doi.org/10.1158/1078-0432.CCR-06-2149.

24. Tang, C., Guo, J., Chen, H., Yao, C.J., Zhuang, D.X., Wang, Y., Tang, W.J., Ren, G., Yao, Y., Wu, J.S., et al. (2015). Gene mutation profiling of primary glioblastoma through multiple tumor biopsy guided by 1H-magnetic resonance spectroscopy. Int. J. Clin. Exp. Pathol. *8*, 5327–5335.

25. Binder, Z.A., Thorne, A.H., Bakas, S., Wileyto, E.P., Bilello, M., Akbari, H., Rathore, S., Ha, S.M., Zhang, L., Ferguson, C.J., et al. (2018). Epidermal Growth Factor Receptor Extracellular Domain Mutations in Glioblastoma Present Opportunities for Clinical Imaging and Therapeutic Development. Cancer Cell *34*, 163–177.e7. https://doi.org/10.1016/j.ccell.2018.06.006.

26. Alakus, H., Babicky, M.L., Ghosh, P., Yost, S., Jepsen, K., Dai, Y., Arias, A., Samuels, M.L., Mose, E.S., Schwab, R.B., et al. (2014). Genome-wide mutational landscape of mucinous carcinomatosis peritonei of appendiceal origin. Genome Med. *6*, 43. https://doi.org/10.1186/gm559.

27. Zhu, Y., Guignard, F., Zhao, D., Liu, L., Burns, D.K., Mason, R.P., Messing, A., and Parada, L.F. (2005). Early inactivation of p53 tumor suppressor gene cooperating with NF1 loss induces malignant astrocytoma. Cancer Cell *8*, 119–130. https://doi.org/10.1016/j.ccr.2005.07.004.

28. Wang, Q., Hu, B., Hu, X., Kim, H., Squatrito, M., Scarpace, L., deCarvalho, A.C., Lyu, S., Li, P., Li, Y., et al. (2017). Tumor Evolution of Glioma-Intrinsic Gene Expression Subtypes Associates with Immunological Changes in the Microenvironment. Cancer Cell *32*, 42–56.e6. https://doi.org/10.1016/j.ccell.2017.06.003.

29. Ozawa, T., Riester, M., Cheng, Y.K., Huse, J.T., Squatrito, M., Helmy, K., Charles, N., Michor, F., and Holland, E.C. (2014). Most human non-GCIMP glioblastoma subtypes evolve from a common proneural-like precursor glioma. Cancer Cell *26*, 288–300. https://doi.org/10.1016/j.ccr.2014.06.005.

30. Jagani, Z., Mora-Blanco, E.L., Sansam, C.G., McKenna, E.S., Wilson, B., Chen, D., Klekota, J., Tamayo, P., Nguyen, P.T.L., Tolstorukov, M., et al. (2010). Loss of the tumor suppressor Snf5 leads to aberrant activation of the Hedgehog-Gli pathway. Nat. Med. *16*, 1429–1433. https://doi.org/10.1038/nm.2251.

31. Zhang, M., Gao, L., Ye, Y., and Li, X. (2022). Advances in glioma-associated oncogene (GLI) inhibitors for cancer therapy. Invest. New Drugs *40*, 370–388. https://doi.org/10.1007/s10637-021-01187-2.

32. Obasaju, P., Brondon, J., Mir, S., Fordham, L.A., Lee, S., and Blatt, J. (2018). Somatic PTPN11 Mutation in a Child With Neuroblastoma and Protein Losing Enteropathy. J. Pediatr. Hematol. Oncol. *40*, 328–330. https://doi.org/10.1097/MPH.0000000000000903.

33. Neftel, C., Laffy, J., Filbin, M.G., Hara, T., Shore, M.E., Rahme, G.J., Richman, A.R., Silverbush, D., Shaw, M.L., Hebert, C.M., et al. (2019). An Integrative Model of Cellular States, Plasticity, and Genetics for Glioblastoma. Cell *178*, 835–849.e21. https://doi.org/10.1016/j.cell.2019.06.024.

34. Ngo, M.T., and Harley, B.A.C. (2019). Perivascular signals alter global gene expression profile of glioblastoma and response to temozolomide in a gelatin hydrogel. Biomaterials *198*, 122–134. https://doi.org/10.1016/j.biomaterials.2018.06.013.

35. Jung, E., Osswald, M., Ratliff, M., Dogan, H., Xie, R., Weil, S., Hoffmann, D.C., Kurz, F.T., Kessler, T., Heiland, S., et al. (2021). Tumor cell plasticity, heterogeneity, and resistance in crucial microenvironmental niches in glioma. Nat. Commun. *12*, 1014. https://doi.org/10.1038/s41467-021-21117-3.

36. Wang, J., Xu, S.L., Duan, J.J., Yi, L., Guo, Y.F., Shi, Y., Li, L., Yang, Z.Y., Liao, X.M., Cai, J., et al. (2019). Invasion of white matter tracts by glioma stem cells is regulated by a NOTCH1-SOX2 positive-feedback loop. Nat. Neurosci. *22*, 91–105. https://doi.org/10.1038/s41593-018-0285-z.

37. Moran, C.M., Myers, C.T., Lewis, C.M., and Krieg, P.A. (2012). Hedgehog regulates angiogenesis of intersegmental vessels through the VEGF signaling pathway. Dev. Dyn. *241*, 1034–1042. https://doi.org/10.1002/dvdy.23795.

38. Anderson, K.J., Tan, A.C., Parkinson, J., Back, M., Kastelan, M., Newey, A., Brewer, J., Wheeler, H., Hudson, A.L., Amin, S.B., et al. (2020). Molecular and clonal evolution in recurrent metastatic gliosarcoma. Cold Spring Harb. Mol. Case Stud. *6*, a004671. https://doi.org/10.1101/mcs.a004671.

39. Lee, J.K., Wang, J., Sa, J.K., Ladewig, E., Lee, H.O., Lee, I.H., Kang, H.J., Rosenbloom, D.S., Camara, P.G., Liu, Z., et al. (2017). Spatiotemporal genomic architecture informs precision oncology in glioblastoma. Nat. Genet. *49*, 594–599. https://doi.org/10.1038/ng.3806.

40. Kim, H., Zheng, S., Amini, S.S., Virk, S.M., Mikkelsen, T., Brat, D.J., Grimsby, J., Sougnez, C., Muller, F., Hu, J., et al. (2015). Whole-genome and multisector exome sequencing of primary and post-treatment glioblastoma reveals patterns of tumor evolution. Genome Res. *25*, 316–327. https://doi.org/10.1101/gr.180612.114.

41. Thomsen, M.B.H., Nordentoft, I., Lamy, P., Høyer, S., Vang, S., Hedegaard, J., Borre, M., Jensen, J.B., Ørntoft, T.F., and Dyrskjøt, L. (2016). Spatial and temporal clonal evolution during development of metastatic urothelial carcinoma. Mol. Oncol. *10*, 1450–1460.

https://doi.org/10.1016/j.molonc.2016.08.003.

42. Thomsen, M.B.H., Nordentoft, I., Lamy, P., Vang, S., Reinert, L., Mapendano, C.K., Høyer, S., Ørntoft, T.F., Jensen, J.B., and Dyrskjøt, L. (2017). Comprehensive multiregional analysis of molecular heterogeneity in bladder cancer. Sci. Rep. *7*, 11702. https://doi.org/10.1038/s41598-017-11291-0.

43. Francis, G., and Stein, S. (2015). Circulating Cell-Free Tumour DNA in the Management of Cancer. Int. J. Mol. Sci. *16*, 14122–14142. https://doi.org/10.3390/ijms160614122.

44. Olsson, E., Winter, C., George, A., Chen, Y., Howlin, J., Tang, M.H.E., Dahlgren, M., Schulz, R., Grabau, D., van Westen, D., et al. (2015). Serial monitoring of circulating tumor DNA in patients with primary breast cancer for detection of occult metastatic disease. EMBO Mol. Med. *7*, 1034–1047. https://doi.org/10.15252/emmm.201404913.

45. Bakas, S., Ormond, D.R., Alfaro-Munoz, K.D., Smits, M., Cooper, L.A.D., Verhaak, R., and Poisson, L.M. (2020). iGLASS: imaging integration into the Glioma Longitudinal Analysis Consortium. Neuro Oncol. *22*, 1545–1546. https://doi.org/10.1093/neuonc/noaa160.

46. Lavon, I., Zrihan, D., Zelikovitch, B., Fellig, Y., Fuchs, D., Soffer, D., and Siegal, T. (2007). Longitudinal assessment of genetic and epigenetic markers in oligodendrogliomas. Clin. Cancer Res. *13*, 1429–1437. https://doi.org/10.1158/1078-0432.CCR-06-2050.

47. Sheng, Z., Yu, J., Deng, K., Andrade-Barazarte, H., Zemmar, A., Li, S., Li, N., Yan, Z., Chen, Z., Sun, Y., et al. (2021). Characterizing the Genomic Landscape of Brain Glioma With Circulating Tumor DNA From Tumor In Situ Fluid. Front. Oncol. *11*, 584988. https://doi.org/10.3389/fonc.2021.584988.

STAR★METHODS

KEY RESOURCES TABLE

REAGENT or RESOURCE	SOURCE	IDENTIFIER
Biological samples		
Human glioma tissue and tumor *in situ* fluid (TISF) samples	Department of Neurosurgery, Zhengzhou University People's Hospital, Henan Provincial People's Hospital(Zhengzhou,China)	PRJNA982268
Glioma patients'blood samples	Department of Neurosurgery, Zhengzhou University People's Hospital, Henan Provincial People's Hospital(Zhengzhou,China)	N/A
Chemicals, peptides, and recombinant proteins		
DNA Blood Midi/Mini kit	Qiagen, USA	Cat# 69504
MagMAX Cell-Free DNA Isolation Kit	Thermo Fisher Scientific, USA	Cat# A29319
An process of DNA fragment end repair, PCR amplification	Beijing Genetron Health Technology Co., Ltd. (China, Beijing)	N/A
DNeasy Blood &Tissue Kit	Qiagen, USA	Cat# 69506
An 68-gene pane	Beijing Genetron Health Technology Co., Ltd. (China, Beijing)	This paper
Deposited data		
Raw data	This paper	https://dataview.ncbi.nlm.nih.gov/object/PRJNA982268
Analyzed data	This paper	Table S1
Experimental models: Organisms/strains		
Patients: Glioma patients	Department of Neurosurgery, Zhengzhou University People's Hospital, Henan Provincial People's Hospital(Zhengzhou,China)	Tables S1 and S2
Software and algorithms		
Torrent Suite™ Software	Life Technologies	N/A
Variant Caller Plugin v4.4	Life Technologies	N/A
Next GENe® v.2.3.4 software	Soft Genetics, State College, PA	https://softgenetics.com/ RRID:SCR_011859
ANNOVAR	N/A	http://www.openbioinformatics.org/annovar/) RRID:SCR_012821
Other		
Illumina NovaSeq 6000	Illumina, USA	Cat# 20012850

RESOURCE AVAILABILITY

Lead contact

Further information and requests for resources should be directed to and will be fulfilled by the Lead Contact, Xingyao Bu (xingyaob@zzu.edu.cn).

Materials availability

The present study did not generate new unique reagents.

Data and code availability

Datasets supporting the conclusions contained in the present report are included in the manuscript all data and supplemental information. The sequencing data will be publicly available in the NCBI repository (PRJNA982268). More information and examples of acceptable statements and approved repositories

are at https://dataview.ncbi.nlm.nih.gov/object/PRJNA982268. Gene evolution of glioma under stress treatment(NCT05512325) has been registered in https://clinicaltrials.gov/.

Any additional information required to reanalyze the data reported in this manuscript is available from the lead contact upon request.

EXPERIMENTAL MODEL AND SUBJECT PARTICIPANT DETAILS

Patient characteristics

Patients provided written informed consent to participate in the study, and their samples and clinical data were collected for research according to the research proposals approved by the Henan Provincial People's Hospital Institutional Review Board and the committees for ethical review of research at Zhengzhou University (Zhengzhou, China). Tissue and TISF were sampled from 32 Asian patients with relapse glioma, male(18,56%) and female(14,44%), age(52.7 $\pm$14.4). We collected longitudinal genomic profiles of 7 IDH mutation glioma samples and their matched TISF samples after the initial surgery. Among these, 3 patients experienced a local relapse, and 4 patients had a distant relapse, World Health Organization (WHO) grade II-IV. The patients were treated at Henan Provincial People's Hospital from July 2017 to January 2022, China. We collected matched tissue and TISF samples from 25 IDH-wild gliomas. Among these, 22 patients experienced local relapse, and 3 patients had distant relapse.Additionally, 8 patients had multifocal glioma. The histology of all tumors was confirmed by pathological review, according to the WHO 2021 classification of the central nervous system tumors.[46] Clinical information was obtained from medical records, including age at initial diagnosis, gender, tumor location, postoperative therapy, and so on. Tables S1 and S2 show a summary of the respective patient data.

Samples collection

TISF samples were harvested as previously described.[47] We collected a small amount of TISF from glioma patients with the implanted reservoir (Intra-operative retention). Simultaneously, we used genomic DNA from blood samples as a control to remove germline mutations. Fresh tumor tissues were readily accessible to obtain matched baselines and to perform evolution analysis.

METHOD DETAILS

DNA extraction

We used the Cell Free DNA Isolation Kit (Thermo Fisher Scientific; Waltham, MA, USA) to extract Cell-free DNA from liquid samples. While tissue sections from tumor samples were used for genomic DNA extraction with the QIAamp DNA Tissue & Blood Kit (Qiagen; Germantown, MD, USA). Control genomic DNA from the paired blood samples was prepared with the QIAamp DNA Mini Kit (Qiagen) for the purpose of identifying germline mutations. All extractions were carried out according to the respective kit manufacturer's protocol. The DNA quality and quantity were assessed by The QubitAssay Kit (Thermo Fisher Scientific).

ctDNA sequencing

Beijing Genetron Health Technology Co., Ltd. (China, Beijing) performed and analyzed the DNA sequencing based on novaseq high-throughput sequencing platform. Briefly, genomic DNA was PCR amplified using 10ng of genomic DNA primer pool as a template. We designed a high-throughput sequencing panel to identify variants in 68 genes (Genetron Health; Beijing, China), containing major brain tumor-related genes. Sequencing data underwent a primary analysis by the Torrent Suite server 4.4 that used the TMAP algorithm (Life Technologies). Variants were confirmed using the Variant Caller Plugin v4.4 (Life Technologies). An allele fraction of $\geq$ 0.1% and a total of $\geq$ 4 reads were used as criteria to prioritize mutations and were considered existing in the samples. The integrative Genomics Viewer (IGV) was used for variant visualization and to check for possible errors. Copy number variations were determined with the Next GENe® v.2.3.4 software (Soft Genetics, State College, PA). Finally, variant annotation was performed using ANNOVAR, Oncotator and Vep.

QUANTIFICATION AND STATISTICAL ANALYSIS

Mean mutant molecules per milliliter (mMMPM)

Mutant molecules per milliliter (mMMPM) for a specific somatic mutation were calculated as the allele fraction of that variant multiplying by the extracted mass (ng), dividing by the volume (mL), and adjusting for a

factor of 330 haploid human genome equivalents (hGE) per 1 ng. The mMMPM for each TISF sample was calculated based on the predefined somatic variants (single nucleotide variants) identified in the matched tissue sample.

Statistical analysis

Changes in VAFs and SNVs during gene evolution were analyzed. Statistical analysis was performed using GraphPad Prism 8.0 (San Diego, CA, USA). Statistical comparisons between two sample sets were performed with two-sided student's t-test. $P \leq 0.05$ was considered to be statistically significant.